Asian Journal of Chemistry; Vol. 25, No. 5 (2013), 2537-2540

ASIAN JOURNAL OF CHEMISTRY

http://dx.doi.org/10.14233/ajchem.2013.13447

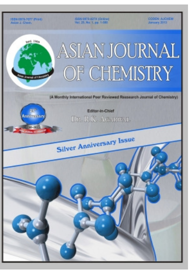

Kinetics of Sulphric Acid Curing-Roasting of Nickel Laterite for Recovering Nickel and Cobalt

QINGHUA TIAN*, DONG LI, XUEYI GUO and WENTANG SHI

School of Metallurgical Science & Engineering, Central South University, Changsha 410083, P.R. China

*Corresponding author: Fax: +86 731 88836207; Tel: +86 731 88877863; E-mail: qinghua@csu.edu.cn

(*Received*: 14 January 2012; *Accepted*: 12 November 2012) AJC-12396

The techniques such as X-ray fluorescence, X-ray diffraction and scanning electron microscope were used to describe the nickel laterite material's crystal structure and morphology. Nickel and cobalt were extracted from nickel laterite by sulphuric acid curing-roasting-leaching process and the kinetics of sulphuric acid curing-roasting was studied. The results show that the sulphuric acid curing of nickel and cobalt accords with the liquid-solid regional reaction model raised by Bagdasarym and the kinetic equation is expressed as $\ln [-\ln (1-\alpha)] = \ln k + n \ln t$. The activation energies are determined to be 21.45 kJ/mol for nickel and 34.81 kJ/mol for cobalt, respectively which are characteristic for an internal diffusion controlled process.

Key Words: Nickel laterite, Sulphuric acid curing, Roasting, Kinetics, Nickel, Cobalt.

INTRODUCTION

The nickel laterite a type of oxidation ores containing nickel, the nickel reserves of which takes *ca.* 60 % of the global land resources[1]. It mainly distributed in New Caledonia, Australia, the Philippines, Indonesia, Central & South America as well as other countries and regions. According to the statistics, *ca.* 40 % nickel production throughout the world came from the nickel laterite in the year of 2003, with the rapid development of the nickel laterite project in recent years, the ratio promises to reach above 50 % due to 2012[2].

Up to now, the treatment progresses of nickel laterite can be classified into pyrometallurgy and hydrometallurgy process. The pyrometallurgy process mainly include ferronickel production by reductive roasting[3] and nickel matt production by reductive sulphuric roasting[4], which is suitable for the treatment of nickel laterite in the humus layer with high-magnesium and low-iron content. While, the hydrometallurgy processes comprise of reductive roasting-ammonia leaching process[5], high-pressure acid leaching process[6], atmospheric pressure acid leaching process[7] and sulphuric acid curing-roasting-leaching process[8,9]. The reductive roasting-ammonia leaching process was first applied to the nickel laterite treatment industrially with the advantages of mature industrial art and high nickel recovery, meanwhile, the disadvantages are complex flow and low cobalt recovery. The high-pressure acid leaching process is of high nickel and cobalt recovery but rigorous operating conditions and high maintenance charges. The atmospheric pressure acid leaching is of short process and easy operation, but the acid consumption is large and the high iron recovery inhibited the downstream processing of the leachate.

The principle of the sulphuric acid curing-roasting-leaching process is the extraction of nickel and cobalt by formation of corresponding sulphate using concentrated sulphuric acid react with nickel and cobalt oxide in the ore, then separated with the residue by water leaching[10,11]. This process is easily operated with low acid consumption, high nickel and cobalt and low iron recovery.

This paper is based on the treatment of nickel laterite by sulphuric acid curing-roasting-leaching process. The sulfation kinetics of the nickel and cobalt is investigated, which provides the theoretical instruction for the industrial application of sulphuric acid curing-roasting-leaching process.

EXPERIMENTAL

The nickel laterite was collected from the Tubay region, Mindanao, Philippines. The raw material used in this study was a typical limoniticaterite ore with high iron content and was ground to -80 mesh after drying at 110 ºC. PW-1160 X-ray fluorescence analyzer was used to determine the chemical composition, X-ray diffraction patterns (XRD) were measured on a D/Max-2550 X-ray diffractometer using CuK_α radiation with scanning from 10-85º. Scanning electron microscope (SEM) images were obtained with JSM-6360LV Scanning spectrometer and WFX-130B atomic absorption spectroscopy (AAS) was used to analyse the Ni and Co content in the leachate.

Experimental methods: 10 g nickel laterite was placed in a 100 mL bowl shape porcelain crucible, 2 mL water was added to make the ore moist, then mixed wtih 2.2 mL conc. sulphuric acid (mass fraction of 98 %) for 5 min, roasted in a box resistance furnace (± 1 ºC). The roasting product is leached at room temperature for 10 min, the Ni and Co content in the leachate was analyzed and the recoveries were calculated.

Reaction principle: The reaction, called sulphric acid curing, is the nickel and cobalt oxide in the nickel laterite converted into hydrosoluble sulphate by concentrated sulphuric acid. The sulfation reactions of nickel and cobalt are as follows:

$$NiO + H_2SO_4 = NiSO_4 + H_2O \quad (1)$$

$$CoO + H_2SO_4 = CoSO_4 + H_2O \quad (2)$$

RESULTS AND DISCUSSION

Mineralogy analysis of the nickel laterite: The assay of nickel laterite material is presented in Table-1, the XRD pattern and microscopy structure are shown in Figs. 1 and 2, respectively. From Table-1 it can be seen that the content of nickel, magnesium and silicon is quite low, meanwhile, the grade of iron reaches *ca.* 50 wt. %, which is the typical limonitic laterite ore with high iron and low magnisium content. It is evident in Fig. 1 that the iron is mainly in the form of goethite (FeOOH). Fig. 2 indicates that the nickel laterite particle is basically in ellipse shape with uneven sizes.

TABLE-1
ASSAY OF NICKEL LATERITE MATERIAL

Elements	Content (wt. %)	Elements	Content (wt. %)
Ni	1.11	Mg	0.18
Co	0.18	Si	1.37
Fe	47.74	Zn	0.12
Mn	1,12	Cr	1.04
Al	2.60	Cu	0.01

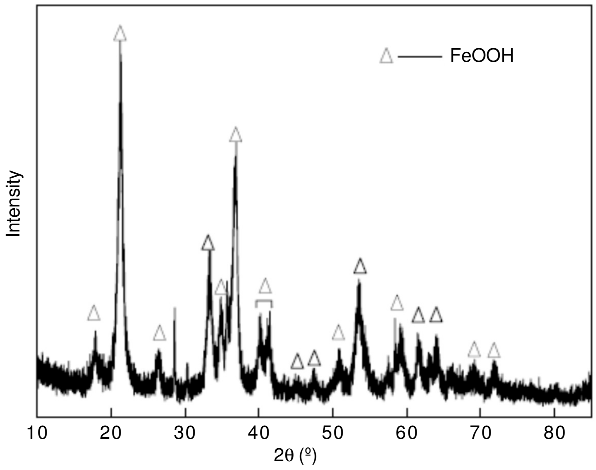

Fig. 1. XRD patterns of the nickel laterite material

TABLE-2
PRESENT MODES OF NICKEL AND
COBALT IN NICKEL LATERITE

Present modes	Distribution proportion (%)			
	Ni	Co	Fe	Mn
Physical adsorption	8.35	75.43	2.24	55.80
Chemical adsorption	2.41	18.01	1.96	21.04
Lattice replacement	89.24	6.56	95.70	23.16

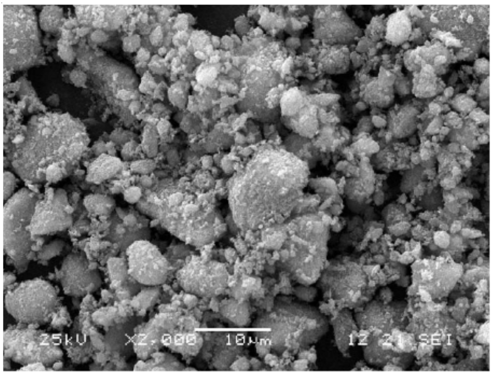

Fig. 2. SEM image of nickel laterite material

The present modes of nickel, cobalt and the coherent elements like iron and manganese were analyzed and presented in Table-2. It is evident that the present modes of nickel and cobalt are different and the present mode of nickel is in close relationship with iron, which is mainly goethite by lattice replacement, the proportion is *ca.* 90 % and a little fraction by adsorption. Cobalt generally coexist with manganese, whose fraction of above 75 % is in the gap between the goethite particles by physical adsorption, at the same time, a little fraction is by chemical adsorption and lattice replacement.

Kinetic curves of nickel and cobalt sulfation: Fig. 3 presented the sulfation kinetic curves of the nickel laterite at the temperatures ranging from 300-750 ºC. In the low temperature region from 300-600 ºC the sulfation degree of nickel increases with the extention of roasting time and the sulfation process approximately completed in *ca.* 0.5 h. This kinetic curves accords with the characteristics of the typical multiphase liquid/solid reaction[12], including the acceleration stage and completion stage. Curves in the acceleration stage indicates the rapid increase of reaction rate with the extention of time, which is also called the autocatalysis stage, since the enlarged reaction interface of sulfation plays a catalytic role with the increase of reaction time. Meanwhile, the curves in the completion stage show that the reaction rate slows down with the extention of time, which is due to the maximizing frontiers of the sulfation interface. The reaction is inhibited with the shrink of the reaction interface and almost completed, which is called the narrowing stage of reaction interface. At the same time, the sulfation rate as well as the sulfation degree of nickel increases with the elevation of the roasting temperature, since the elevated temperature favors the internal diffusion of sulphuric acid to the interior of the solid particle, meanwhile shortens the time reaching sulfation maximizing.

In the high temperature region of above 600 ºC the sulfation rate of nickel increases rapidly in a short time, but decreases with the elevated temperature and further extension of time, meanwhile, the maximizing sulfation degree decreases. On the one hand, the sulfation rate slows down with the shrink of reaction interface, on the other hand, at high temperature, a competitive relationship forms between the sulfation of nickel and the decomposition of nickel sulphate, since the nickel sulphate decomposes into nickel oxide at about 630-670 ºC, *i.e.*:

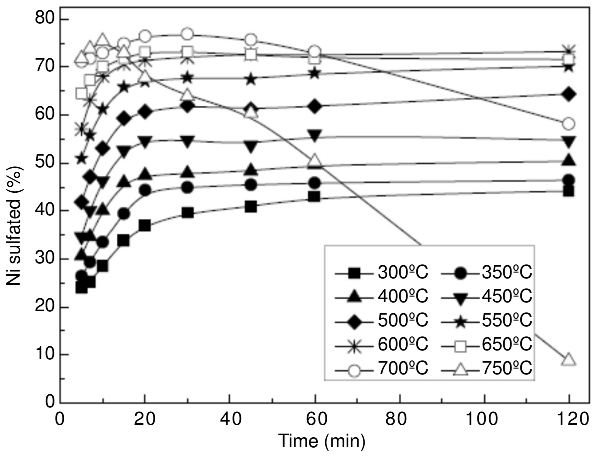

Fig. 3. Dynamic curves of nickel sulfation

$$NiSO_4 = NiO + SO_3 \uparrow \qquad (3)$$

Fig. 4 presents the sulfation kinetic curves of cobalt in the nickel laterite in the temperature range of 300-750 ºC. The kinetic curves of cobalt sulfation are similar with the ones of nickel. Reactions in the low temperature range of 300-600 ºC also accords with the characteristics of the typical multi-phase liquid/solid reaction, as well as the competitive relationship between the sulphate of cobalt and decomposition of cobalt sulphate in the high temperature region above 600 ºC (the initial decomposition temperature is between 640 and 690 ºC)[13]. However, the effect of roasting temperature on the sulfation of cobalt is more obvious than on the sulfation of nickel. The maximizing sulfation degree of nickel increases only from 45-75 % with the rise of temperature, but the cobalt increases from *ca.* 35-90 %.

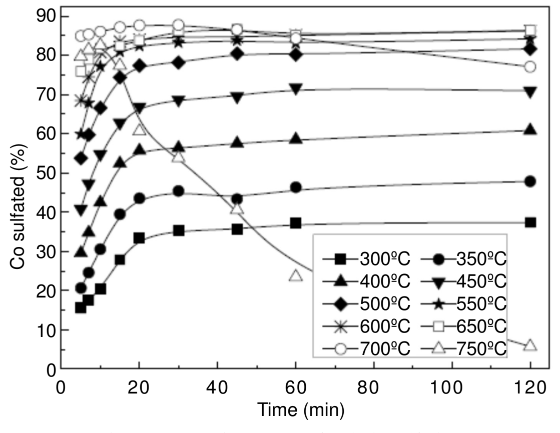

Fig. 4. Dynamic curves of cobalt sulfation

Kinetic type of the nickel and cobalt sulfation: The sulfation kinetic curves of nickel and cobalt at the temperature range of 300-600 ºC accord with the typical multi-phase liquid/solid reaction. (It is noted that due to the poor regularity of the kinetic date at high temperature region of above 600 ºC, they are not analyzed). It accords with the model proposed by Bagdasarym in the year of 1945, which regards to the reaction rate of multi-phase liquid/solid reaction changes from low to quick. The degree of the reaction α can be represented in Erofeev eqution:

$$\alpha = 1 - \exp(-kt^n) \qquad (4)$$

where, α is the reaction degree, *i.e.*, the sulfation proportion of the nickel and cobalt, k is the reaction rate constant, t is the reaction time, n is the function of the crystalline properties and geometry in the ore, which do not change with the variation of the leaching conditions. When n < 1, it accords with the reaction type of high initial reaction rate and decrease with the extention of time[14].

Take napierian logarithm on both sides of eqn. 4, then comes with:

$$\ln[-\ln(1-\alpha)] = \ln k + n \ln t \qquad (5)$$

The sulfation proportion of nickel and cobalt at different time under various temperature into eqn. 5, the lnt *versus* ln (-ln (1-α)) diagrams were plotted (Figs. 5 and 6). It can be seen that ln t is in linear relation with ln [-ln (1-α)] in the sulfation process, which implies that the kinetics of sulfation accords with the model proposed by Bagdasarym and the sulfation rate can be expressed by Erofeev equation. The gradient of the lines in Fig. 5 is between 0.27 and 0.44 with the average value of 0.37 and the gradient of the lines in Fig. 6 is between 0.39 and 0.53 with the average value of 0.48.

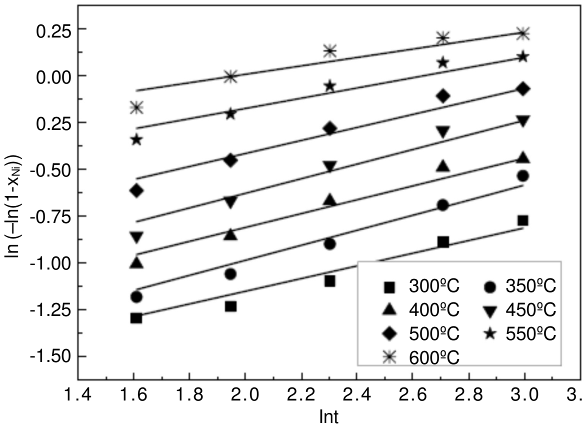

Fig. 5. Curves of ln [-ln (1- α)] to ln t for nickel sulfation

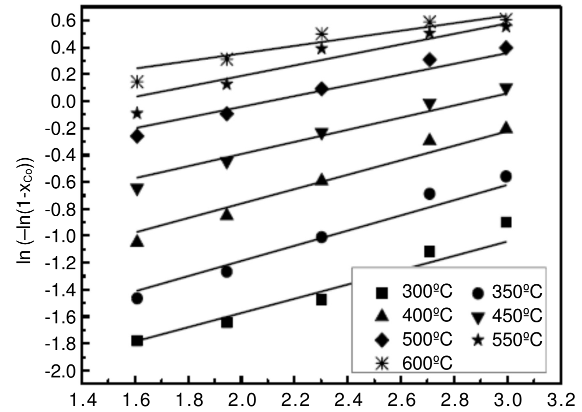

Fig. 6. Curves of ln [-ln (1- α)] to ln t for cobalt sulfation

Apparent activation energy and controlling procedure of the reaction: The reaction rate constant is in function relation with temperature. The effect of temperature on the reaction rate constant is expressed in Arrhenius equation:

$$k = A_0 \exp -\left(\frac{E_0}{RT}\right) \tag{6}$$

or

$$\ln k = \ln A_0 - \left(\frac{E_0}{RT}\right) \tag{7}$$

where, A_0 is the frequency factor, E_0 is the apparent activation energy of the reaction.

It can be seen in eqn. 5 that the intercept of the lines in Figs. 5 and 6 is ln k. The ln k *versus* 1/T diagram was plotted according to eqn. 7 and the apparent activation energy of the sulfation could be obtained through the gradient of the lines. Fig. 7 representes the relation graph of lnk and 1/T of nickel and cobalt sulfation, the apparent activation energy E_0 of nickel and cobalt were calculated as 21.45 and 34.81 kJ/mol, respectively. At the same time, two A_0 values can be obtained by the intercept on the Y-axis in Fig. 7, therefore, the function of the sulfation rate constant k_{Ni}, k_{Co} and the temperature are expressed in eqns. 8 and 9:

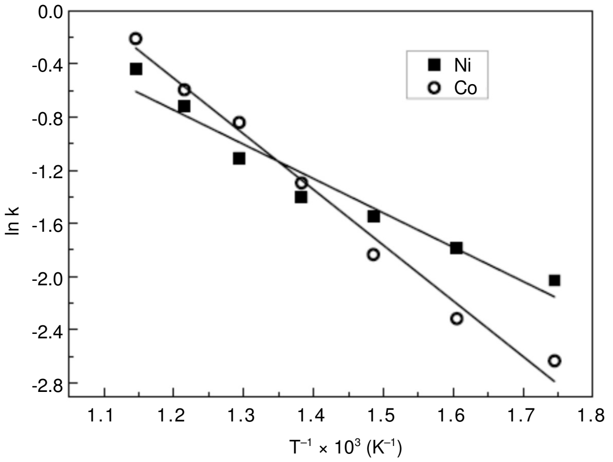

Fig. 7. Curves of ln k to 1/T for nickel and cobalt sulfation

$$k_{Ni} = 10.48 \times \exp\left(\frac{-2.58 \times 10^3}{T}\right) \tag{8}$$

$$k_{Co} = 91.61 \times \exp\left(\frac{-4.19 \times 10^3}{T}\right) \tag{9}$$

The temperature coefficient of the reaction rate constant refers to the magnification of reaction constant with the temperature elevation of each 10 ºC[15]. The kinetic controlling process of the chemical reactions can be distinguished by the temperature coefficient of the reaction constant. For diffusion controlling process, the temperature coefficient is generally 1.0-1.6 and 2 for chemical reaction controlling process. The sulfation rate constant of nickel and cobalt can be calculated to be 1.05 and 1.09 by eqns. 8 and 9, respectively, therefore, the rate control process belongs to internal diffusion control kinetically.

Conclusion

Using concentrated sulphuric acid as reactants, nickel and cobalt was extracted from the low-grade nickel laterite by sulphuric acid curing-roasting process and the sulfation degree reached 75 and 90 %, respectively. In the temperature range of 300-600 ºC, the kinetic curves of nickel and cobalt sulfation in the nickel laterite ore belongs to the typical multi-phase liquid/solid regional reaction. The sulfation rate and degree can be increased by elevating the roasting temperature. The kinetic of sulfation process accords with the model proposed by Bagdasarym, the data of which fits quite well with the equation $\ln(-\ln(1-\alpha)) = \ln k + n \ln t$. The apparent activation energy of nickel and cobalt sulfation is 21.45 and 34.81 kJ/mol, respectively in addition, the sulfation process is controlled by internal diffusion.

ACKNOWLEDGEMENTS

This work was financially supported by National Natural Science Foundation of China (Project No. 51104181), China Postdoctoral Science Foundation (Project No. 20110491279) and Natural Science Foundation of Hunan (Project No. 11JJ4048).

REFERENCES

1. D. Kempthorne and D.M. Myers, Mineral Commodity Summaries, US Geological Survey. Washington, pp. 143-154 (2010).
2. D.D. Ashok, W.G. Bacon and C.O. Robert, The Past and the Future of Nickel Laterites, International Convention, Canada (2004).
3. Z. Liu, H. Yang and Q. Li, Nonferrous Metals (Extractive Metallurgy), 2, 2 (2010).
4. D. Georgiou and V.G. Papangelakis, *Hydrometallurgy*, **49**, 23 (1998).
5. M. Zuniga, F. Parada and E. Asselin, *Hydrometallurgy*, **104**, 260 (2010).
6. B.K. Loverday, *Miner. Eng*., **21**, 533 (2008).
7. W. Luo, Q. Feng and L. Ou, G. Zhang and Y. Lu, *Hydrometallurgy*, **96**, 171 (2009).
8. X. Guo, D. Li, K.H. Park, Q. Tian and Z. Wu, *Hydrometallurgy*, **99**, 144 (2009).
9. D. Li, K.H. Park, Z. Wu and X. Guo, *Trans. Nonferrous Met. Soc. China*, **20**, s92 (2010).
10. Y.V. Swamy, B.B. Kar and J.K. Mohanty, *Hydrometallurgy*, **69**, 89 (2003)
11. R.G. McDonald and B.I. Whittington, *Hydrometallurgy*, **91**, 35 (2008).
12. Q.Y. Han, Dynamics in the Process of Metallurgy, Metallurgy Industry Press, Beijing, pp. 49-54 (1983).
13. H. Tagawa, *Thermochim. Acta*, **80**, 23 (1984).
14. Y.-F. Chang, X.-J. Zhai, Y. Fu, B.-C. Li and T.-A. Zhang, *J. Mol. Sci*., **24**, 241 (2008) (In Chinese).
15. M.-R. Tu and J. Zhou, *Chem. Eng*., **23**, 62 (1995) (In Chinese).